AIAA JOURNAL
Vol. 37, No. 10, October 1999

Active Control of Sound Fields from Plates in Flow by Piezoelectric Sensor/Actuator

Seung Jo Kim* and Kyung Yeol Song†
Seoul National University, Seoul 151-742, Republic of Korea

The objective is to control the sound fields induced by vibrating structures in flow by piezoelectric sensors and actuators. When thin structures such as plates are vibrating in a flow, the fluid loading effects lead to some important changes in the acoustic field and the structural vibration and cannot be neglected. The vibration of plate structures and the sound fields are analyzed using the finite element and the boundary element methods. It is found that some specific modes radiate sound very well compared with the other modes. Because the number of modes that can be controlled simultaneously is limited, the selection of controlled modes is prerequisite. For structural acoustic control, the well-radiating modes, namely, the modes contributing most to far-field sound radiation, should be selected as the controlled modes. Radiation efficiency is used as a reference for the selection of controlled modes. The optimal placement of the piezoceramic material (lead zirconate titanate; PZT) actuators and the optimal electrode shape of polyvinylidene fluoride sensors are determined by a genetic algorithm to minimize the well-radiating modes and to avoid the observation and control spillover. A linear quadratic Gaussian controller is designed to estimate the controlled modes from sensor output and to minimize the performance index. The result shows that global noise reduction can be realized by using the method.

Nomenclature

A	= surface area of plate
$\boldsymbol{A}_c$	= control matrix of controlled modes
$\boldsymbol{B}_c$	= input matrix of controlled modes
C	= speed of sound of a mean flow
$\boldsymbol{C}_c$	= output matrix of controlled modes
$\boldsymbol{C}_u$	= output matrix of uncontrolled modes
$\boldsymbol{D}_c$	= diag$\{2\zeta_i\omega_i\}$; here the ith mode is controlled
$\boldsymbol{F}_d$	= force vector of disturbance
$\boldsymbol{F}_p$	= force vector of fluid loading
G	= Green's function for subsonic flow
$\boldsymbol{K}$	= stiffness matrix of plate
$\boldsymbol{K}_c$	= linear quadratic regulator controller gain
$\boldsymbol{K}_f$	= Kalman filter gain
M	= Mach number of a mean flow
$\boldsymbol{M}$	= mass matrix of plate
$\boldsymbol{P}_a$	= actuator force vector
$\boldsymbol{P}_s$	= sensing force vector of polyvinylidene fluoride elements
$\boldsymbol{p}$	= acoustic pressure vector
$\boldsymbol{S}$	= sensor electrode shape vector
U	= mean flow speed
U_c	= controller input
u, v, w	= displacements along x, y, and z axes, respectively
$\boldsymbol{u}$	= global displacements vector
V_a	= voltage applied to the actuator
$\boldsymbol{v}_n$	= normal velocity vector
$\langle v_n \rangle^2$	= space-averaged value of square vibration velocity
$\boldsymbol{x}_c$	= controlled state variable vector
$\hat{\boldsymbol{x}}_c$	= estimated state vector
y, y_c	= output of sensors and of controlled modes
$\dot{\alpha}$	= time derivative of α
$\ddot{\alpha}$	= second time derivative of α
α^*	= complex conjugate of α
ζ_i	= viscous damping ratio of ith mode
$\boldsymbol{\eta}$	= modal coordinate vector
$\boldsymbol{\eta}_c$	= controlled modal coordinate vector
$\boldsymbol{\eta}_u$	= uncontrolled modal coordinate vector
$\boldsymbol{\Lambda}$	= eigenvalue matrix
$\boldsymbol{\Lambda}_c$	= eigenvalue matrix of controlled mode
$\boldsymbol{\Lambda}_u$	= eigenvalue matrix of uncontrolled mode
Π	= radiated sound power
ρ	= density of a mean flow
σ	= radiation efficiency
$\boldsymbol{\Phi}$	= modal matrix
$\boldsymbol{\Phi}_c$	= modal matrix of controlled modes
$\boldsymbol{\Phi}_u$	= modal matrix of uncontrolled modes
φ	= potential function
$\varphi_x \varphi_y$	= rotational angle along x and y axes, respectively

I. Introduction

SOUND radiation and transmission from vibrating structures is an important problem for engineering applications, e.g., the reduction of noise transmission into an aircraft cabin. Considerable effort has been devoted to active control techniques to reduce low-frequency sound radiated from vibrating structures because passive control techniques are likely to increase the weight of structures and are not effective at low frequencies. For structurally radiated or transmitted noise, the sound field is directly coupled to the structural motion. Therefore, it is efficient to directly apply the control inputs to the vibrating structure to suppress the radiated sound fields.[1]

As the speed of aircraft is increased, the effect of flow on the acoustic field and structural vibration becomes more important and cannot be neglected.[2] When thin structures, such as plates or shells, are vibrating in a flow, fluid loading effects cannot be neglected and lead to changes in the acoustic field and structural vibrations compared with conditions without flow as follows: first, by the reduction in natural frequencies[2] and second, by the increase in radiation efficiency. On the other hand, the structural mode shapes remain almost unchanged when the fluid is not bounded by the structure.[3] Therefore, a specific control strategy is needed to reduce noise from structures in a flow.

Piezoelectric materials, such as lead zirconate titanate (PZT) and polyvinylidene fluoride (PVDF), are being widely used as distributed sensors and actuators in control applications, especially in the fields of structural vibration control and active structural acoustic control. PVDF has desirable properties such as flexibility, softness, responsiveness, and light weight. PVDF also has relatively easy electrode pattern shaping in addition to flexibility. Studies of PVDF have mainly been concerned with sensor design. Compared with

Presented as Paper 98-1800 at the AIAA/ASME/ASCE/AHS/ASC 39th Structures, Structural Dynamics, and Materials Conference, Long Beach, CA, 20–23 April 1998; received 27 July 1998; revision received 7 February 1999; accepted for publication 7 February 1999.

*Professor, Department of Aerospace Engineering. Member AIAA.
†Research Assistant, Department of Aerospace Engineering.

PVDF, PZT requires a large actuating force, and attention must be given to positioning and sizing PZT. Therefore, there has been much research on the use of PVDF and PZT as a sensor and an actuator, respectively.

A new approach is suggested for the design of piezoelectric sensors and actuators to control sound fields induced by vibrating plates in flow. The vibration of the plate structure by a piezoelectric material and the sound radiation from the plate are analyzed using the coupled finite element method (FEM) and boundary element method (BEM). It is found that some specific modes are very effective radiators compared with the other modes. Because the number of modes that can be controlled simultaneously is limited, the selection of controlled modes is critical. For vibration control, lower modes should be suppressed in consecutive order, e.g., first to third modes. On the other hand, for structural acoustic control, the well-radiating modes (the modes contributing to the far-field sound radiation) should be controlled modes, e.g., first, fourth, and seventh modes. Radiation efficiency is used as a reference for the selection of controlled modes. Optimal electrode shape of the PVDF sensor and optimal placement of the PZT actuators are determined to control these well-radiating modes by using a genetic algorithm. A linear quadratic Gaussian (LQG) control law has been applied to the integrated structure. Numerical analysis is carried out for the sound fields from a simply supported plate structure. Piezoelectric sensor and actuators are designed to control these sound fields.

II. Formulation of the System Equation

Finite Element Analysis of Plate Structure

Figure 1 shows a schematic view of the structure considered. The host structure and the piezoelectric sensor and actuators are vibrating under the excitation of the disturbance. On one side of the plate, the fluid moves at a mean velocity U. This fluid affects the response of the plate. Because of the disturbances, the plate radiates the acoustic power toward the other side. The design of piezoelectric sensor and actuator to minimize this acoustic power is the objective of the present study. The FEM is used to model the plate structure with the piezoelectric sensor and actuator. Nine-node Reissner–Mindlin plate elements have been used. Each node has five degrees of freedom (u, φ_x, v, φ_y, and w), as shown in Fig. 2. The structure is described as follows:

$$\boldsymbol{M}\ddot{\boldsymbol{u}} + \boldsymbol{K}\boldsymbol{u} = \boldsymbol{P}_a V_a + \boldsymbol{F}_d + \boldsymbol{F}_p \tag{1}$$

where $\boldsymbol{M}$ and $\boldsymbol{K}$ are global mass and stiffness matrices, respectively, $\boldsymbol{P}_a$ is the actuation force vector of the piezoelectric actuator, $\boldsymbol{F}_d$ is the disturbance, $\boldsymbol{F}_p$ is the fluid loading vector by the fluid pressure, and $\boldsymbol{u}$ is the nodal displacement.

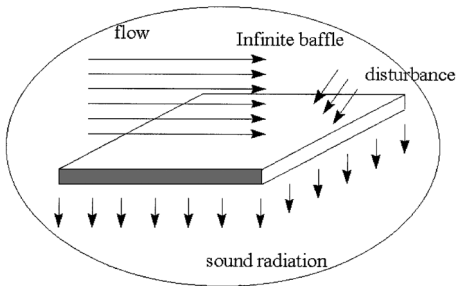

Fig. 1 Integrated plate structure supported on an infinite baffle.

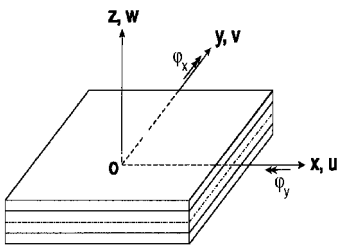

Fig. 2 Degrees of freedom at a node.

Equation (1) is transformed by using the following modal coordinate transformation:

$$\boldsymbol{u} = \boldsymbol{\Phi}\boldsymbol{\eta} \tag{2}$$

Assuming that eigenvectors are normalized as follows:

$$\boldsymbol{\Phi}^T\boldsymbol{M}\boldsymbol{\Phi} = \boldsymbol{I}, \qquad \boldsymbol{\Phi}^T\boldsymbol{K}\boldsymbol{\Phi} = \boldsymbol{\Lambda} \tag{3}$$

the transformed modal coordinate equation can be written as

$$\ddot{\boldsymbol{\eta}} + \boldsymbol{\Lambda}\boldsymbol{\eta} = \boldsymbol{\Phi}^T\boldsymbol{P}_a V_a + \boldsymbol{\Phi}^T(\boldsymbol{F}_d + \boldsymbol{F}_p) \tag{4}$$

In Eq. (4), Λ is the matrix composed of the eigenvalues of Eq. (1), and $\boldsymbol{\Phi}^T\boldsymbol{P}_a$ is defined as the modal control force per unit voltage and is used in the objective function for the design of sensors and actuators. According to the reciprocal relationship between the piezoelectric sensor and actuator,[4] the charge induced in the piezoelectric sensor is

$$q = \boldsymbol{P}_a^T\boldsymbol{u} \equiv \boldsymbol{P}_s^T\boldsymbol{u} \tag{5}$$

where subscript s is the sensor.

Equation of the Acoustic System

The acoustic pressure in the acoustic domain induced by the vibrating plate in the baffle can be facilitated by introducing potential function φ, which satisfies the following equation[5]:

$$\left[\nabla^2 - \frac{1}{C^2}\left(-i\omega + U\frac{\partial}{\partial x}\right)^2\right]\varphi(x, y, z, \omega) = 0 \tag{6}$$

subject to the boundary conditions

$$\frac{\partial\varphi}{\partial z} = \begin{cases}\left(-i\omega + U\dfrac{\partial}{\partial x}\right)w(x, y, \omega), & x \in A\\ 0, & \text{otherwise}\end{cases} \tag{7}$$

The potential function can be obtained by introducing Green's function[5]

$$\varphi(x, y, z, \omega) = \int_A G(x, y, z \mid x', y', 0)\left(-i\omega + U\frac{\partial}{\partial x'}\right) \times w(x', y', \omega)\,dx'\,dy' \tag{8}$$

The quantity G in Eq. (8) is Green's function for a subsonic flow, which is given by[5]

$$G(x, y, z \mid x', y', 0) = -\frac{e^{ikR_1}}{2\pi(1 - M^2)^{\frac{1}{2}}R_2} \tag{9}$$

where R_1 and R_2 are defined as follows:

$$R_1 = \sqrt{\frac{1}{1 - M^2}(x - x')^2 + (y - y')^2}$$

$$R_2 = \frac{(x - x')M + \sqrt{(x - x')^2 + (1 - M^2)(y - y')^2}}{1 - M^2} \tag{10}$$

The radiated acoustic pressure in the frequency domain can now be written as[5]

$$p(x, y, z, \omega) = -\rho\left(-i\omega + U\frac{\partial}{\partial x}\right)\varphi(x, y, z, \omega) \tag{11}$$

where ρ is the fluid density and p is the acoustic pressure in the frequency domain. Equation (11) becomes the Helmholz equation when the mean flow U is zero.

When Eq. (11) is discretized with Eq. (7), using the boundary element method, we obtain the matrix equation as

$$\boldsymbol{p} = \boldsymbol{G}\boldsymbol{v}_n \tag{12}$$

where $\boldsymbol{p}$ and $\boldsymbol{v}_n$ are the vectors containing the acoustic pressure and the normal velocity at nodal points, respectively. A four-node quadrilateral element is used for the discretization. The transformation method, which divides the quadrilateral element domain into two triangular domains, is used for the singular integration in the diagonal term of the matrix $\boldsymbol{G}$ (Ref. 6).

Sound Power and Radiation Efficiency

For global minimization of sound fields induced by vibrating plates, sound power and radiation efficiency are used as a measure of the effectiveness of sound radiation. Radiated sound power is defined as the integration of the sound intensity over the surface of the vibrating plate[7]:

$$\Pi = \frac{1}{2}\int_A Re\left[p^* v_n\right] \mathrm{d}A \tag{13}$$

Radiation efficiency is defined as the ratio of the average acoustic power radiated per unit area of a vibrating surface to the average acoustic power radiated per unit area of a piston that is vibrating with the same average mean square velocity[3]:

$$\sigma = \frac{\Pi}{\Pi_0} = \frac{\Pi}{\frac{1}{2}\rho_0 C A\left\langle v_n^2\right\rangle} \tag{14}$$

Radiation efficiency is used as a reference for the selection of controlled modes.

III. Design of Sensor, Actuator, and LQG Controller

Selection for Controlled Modes

It is well known that the best way to suppress sound fields induced by vibrating structures is to suppress all of their modes. However, the selection for controlled modes is prerequisite because the number of modes that can be controlled simultaneously is limited. Also, for structural acoustic control, the objective is not necessarily to control all of the modes on the plate but to control the well-radiating modes, or those modes contributing most to far-field sound radiation.[8] Therefore, in structural acoustic control, well-radiating modes should be selected for the controlled modes. Radiation efficiency is used as a reference when selecting controlled modes.

Sensor Design

In most investigations of the control of sound fields, microphones are used as sensors in the control approaches.[9–11] However, the use of a pressure sensor, such as a microphone, is excluded here because it is impractical to use a microphone located in the far field, for example, to reduce the cabin noise of aircraft. Also, for the development of an intelligent structure, sensors as well as actuators must be an integral part of the structure. This is the reason that PVDF polymer is used as a sensor.

PVDF has good flexibility, softness, and responsiveness, which enhance its use as a sensor for an intelligent structure. Also, PVDF has the advantage of the relative ease of electrode pattern shaping, in addition to flexibility and light weight. Past studies of PVDF have mainly considered sensor design. For efficient design of piezoelectric sensors in this research, PVDF is segmented into some electrode elements. Some parts of these electrode segments are removed to maximize the observability of controlled modes and to minimize the observation spillover of residual modes.[12] Figure 3 shows four electrode segments in one plate element as used in the study. The sensing force of a PVDF element in Fig. 3 is

$$\boldsymbol{P}_s = \sum_i \boldsymbol{S}(i)\boldsymbol{P}_s^{(i)} = 1 \times \left(\boldsymbol{P}_s^{(1)} + \boldsymbol{P}_s^{(2)} + \boldsymbol{P}_s^{(4)}\right) + 0 \times \boldsymbol{P}_s^{(3)} \tag{15}$$

where

$$\boldsymbol{S}(i) = \begin{cases} 1, & \text{if the electrode segment is on} \\ 0, & \text{if the electrode segment is off} \end{cases}$$

The $\boldsymbol{S}$ vector in Eq. (15) determines the electrode shape pattern of the PVDF sensor and is used as the present design variable. The electrode in the segment selected to be off is removed by chemical etching. The performance index to be maximized is

$$\text{maximize:} \quad \frac{\min\left(\left|\boldsymbol{\Phi}_c^T \boldsymbol{P}_s\right|\right)}{\max\left(\left|\boldsymbol{\Phi}_u^T \boldsymbol{P}_s\right|\right)} \tag{16}$$

where $\boldsymbol{\Phi}_c^T \boldsymbol{P}_s$ and $\boldsymbol{\Phi}_u^T \boldsymbol{P}_s$ are the modal forces for the controlled modes and for the uncontrolled modes, respectively. This performance index is introduced to maximize the minimum of the modal forces for the controlled modes and to minimize the maximum of the modal forces for the uncontrolled modes.

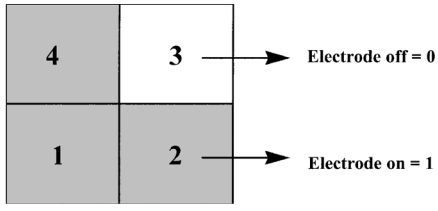

Fig. 3 Nine-point plate element with four electrode segments.

Actuator Design

To suppress vibration and acoustic radiation of plates in flow, a powerful actuating force is necessary, and PZT satisfies this requirement. In the design of actuators, the optimal placement of PZT actuators is calculated to maximize the actuating force for the well-radiating modes and to minimize the control spillover, when the number and the size of PZT actuators are given. The boundary of the PZT is assumed to be the same as that of the elements in the study. When an element is covered with PZT actuators, that element turns on. When an element is not covered with PZT actuators, that element turns off. This assumption is introduced to facilitate finite element analysis of the plate structure including PZT actuators. Because of its large mass and stiffness, the effect of PZT on the structural property of the host structure cannot be neglected. The on and off of each element is determined by using the genetic algorithm. The performance index to be maximized is

$$\text{maximize:} \quad \frac{\min\left(\left|\boldsymbol{\Phi}_c^T \boldsymbol{P}_a\right|\right)}{\max\left(\left|\boldsymbol{\Phi}_u^T \boldsymbol{P}_a\right|\right)} \tag{17}$$

where $\boldsymbol{\Phi}_c^T \boldsymbol{P}_a$ and $\boldsymbol{\Phi}_u^T \boldsymbol{P}_a$ are the modal forces for the controlled modes and for the uncontrolled modes, respectively. This performance index is introduced to maximize the minimum of the modal actuating forces for the controlled modes and to minimize the maximum of the modal actuating forces for the uncontrolled modes.

Optimization Method: Genetic Algorithm

The genetic algorithm is used as an optimization method in the design of the piezoelectric sensor and actuator because this algorithm does not require derivative information to get the next generation and can be applied easily to the discontinuous problem, as in the case of the present study.[13] In the case of sensor design, the on and off of electrode segments of each element are determined, whereas in the case of actuator design, the on and off of each element are determined.

Controller Design: LQG Controller

An LQG controller is designed to estimate the controlled modes from the sensor output and to minimize the performance index. The mean flow speed is assumed to be less than the flutter speed. This means that flutter suppression does not have to be considered. For real-time control, it is necessary to limit the size of the controller. We divide the modal vector $\boldsymbol{\eta}$ in Eq. (4) into the controlled modes $\boldsymbol{\eta}_c$ and the uncontrolled modes $\boldsymbol{\eta}_u$:

$$\boldsymbol{\eta} = \begin{bmatrix} \boldsymbol{\eta}_c \\ \boldsymbol{\eta}_u \end{bmatrix} \tag{18}$$

For structural acoustic control, the controlled modes mean the well-radiating modes that should be suppressed. Then the state-space form of the system, which consists of the controlled modes, can be written as

$$\dot{\boldsymbol{x}}_c = \begin{bmatrix} \dot{\boldsymbol{\eta}}_c \\ \ddot{\boldsymbol{\eta}}_c \end{bmatrix} = \begin{bmatrix} \boldsymbol{0} & \boldsymbol{I} \\ -\boldsymbol{\Lambda}_c & -\boldsymbol{D}_c \end{bmatrix} \begin{bmatrix} \boldsymbol{\eta}_c \\ \dot{\boldsymbol{\eta}}_c \end{bmatrix} + \begin{bmatrix} \boldsymbol{0} \\ \boldsymbol{\Phi}_c^T \boldsymbol{P}_a \end{bmatrix} V_a$$
$$= \boldsymbol{A}_c \boldsymbol{x}_c + \boldsymbol{B}_c U_c \tag{19}$$

$$y = \begin{bmatrix} \boldsymbol{P}_s^T \boldsymbol{\Phi}_c & \boldsymbol{P}_s^T \boldsymbol{\Phi}_u & \boldsymbol{0} & \boldsymbol{0} \end{bmatrix} \begin{bmatrix} \boldsymbol{\eta}_c \\ \boldsymbol{\eta}_u \\ \dot{\boldsymbol{\eta}}_c \\ \dot{\boldsymbol{\eta}}_u \end{bmatrix} = \boldsymbol{C}_c \boldsymbol{x}_c + \boldsymbol{C}_u \boldsymbol{x}_u \tag{20}$$

where subscripts c and u are the controlled modes and the uncontrolled modes, respectively. The LQG controller, which is designed to suppress the controlled modes, has the following form[14]:

$$\dot{\hat{\boldsymbol{x}}} = (\boldsymbol{A}_c - \boldsymbol{B}_c\boldsymbol{K}_c - \boldsymbol{K}_f\boldsymbol{C}_c)\hat{\boldsymbol{x}}_c + \boldsymbol{K}_f y$$
$$U_c = V_a = -\boldsymbol{K}_c\hat{\boldsymbol{x}}_c \tag{21}$$

In Eq. (21), $\hat{\boldsymbol{x}}_c$ is the estimated state of $\boldsymbol{x}_c$.

IV. Numerical Example

Radiation Efficiencies of a Simply Supported Aluminum Plate: Verification

To verify the coupled FEM–BEM analysis, the radiation efficiencies of a simply supported aluminum plate on an infinite baffle are calculated at Mach number 0.4. The acoustic medium is air, whose density is 1.21 kg/m^3 and wave velocity is 343 m/s. The plate has dimensions of $0.3 \times 0.2 \times 0.001$ m. The material properties of aluminum are Young's modulus 70 GPa, Poisson's ratio 0.3, and density 2700 kg/m^3. The results from the analytical approach by Chang and Leehey[15] are compared with present results in Fig. 4. Comparison of the results in Fig. 4 shows good agreement.

Control of Sound Fields from a Simply Supported Aluminum Plate in Flow

The acoustic radiation from a simply supported aluminum plate on an infinite baffle and excited by disturbances is calculated at Mach = 0.0–0.4 (Fig. 5). It is estimated that the mean flow speed is less than the flutter speed. The acoustic medium is air, whose density is 1.21 kg/m^3 and wave velocity is 343 m/s. The plate has dimensions of $0.3 \times 0.2 \times 0.001$ m. The material properties of aluminum are Young's modulus 70 GPa, Poisson's ratio 0.3, and density 2700 kg/m^3. The material properties of PZT and PVDF are given in Table 1 (Refs. 16 and 17).

The forcing frequency is assumed to be in the range of 0–600 Hz. The disturbance may be due to engine noise, turbulent boundary layer, etc. (Research on the disturbance is not the objective of the present study.) Therefore, the disturbance is modeled by random harmonic point forces exerted on each node of the plate. When the plate is vibrating in a flow, we can observe the reduction of the natural frequencies from Fig. 5. To select controlled modes, the

Table 1 Material properties of PZT and PVDF[16,17]

Property	PZT	PVDF
E_1, GPa	61.0	3.0
Density, kg/m^3	7700	1780
Thickness, m	2.54×10^{-4}	5.2×10^{-5}
$d31$ (m/m)/(V/m)	1.71×10^{-10}	2.3×10^{-11}
$d32$ (m/m)/(V/m)	1.71×10^{-10}	3.0×10^{-12}

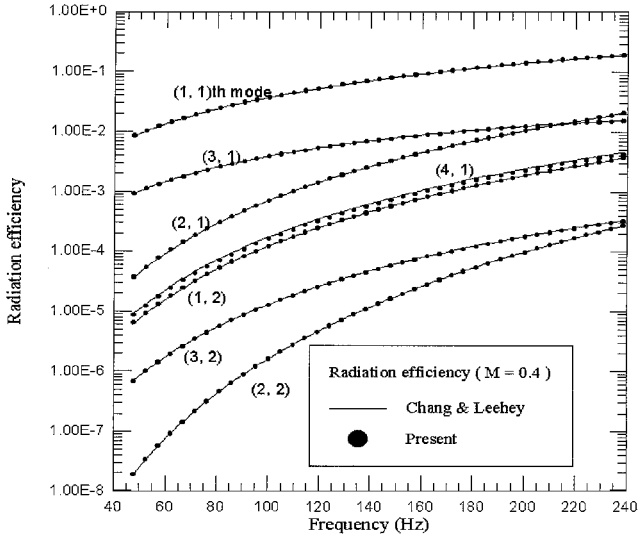

Fig. 4 Radiation efficiency of simply supported isotropic aluminum plate at $M = 0.4$.

Table 2 Natural frequency and radiation efficiency of simply supported aluminum plate with piezoelectric material, $M = 0.0$[a]

Mode	Frequency, Hz	Radiation efficiency
1 (1, 1)	81	$\mathbf{1.375 \times 10^{-2}}$
2 (2, 1)	161	8.745×10^{-4}
3 (1, 2)	260	2.591×10^{-3}
4 (3, 1)	294	$\mathbf{1.630 \times 10^{-2}}$
5 (2, 2)	346	3.537×10^{-4}
6 (3, 2)	478	2.397×10^{-3}
7 (4, 1)	484	$\mathbf{1.296 \times 10^{-2}}$
8 (1, 3)	569	$\mathbf{4.644 \times 10^{-2}}$

[a]Boldfaced values are well-radiating modes.

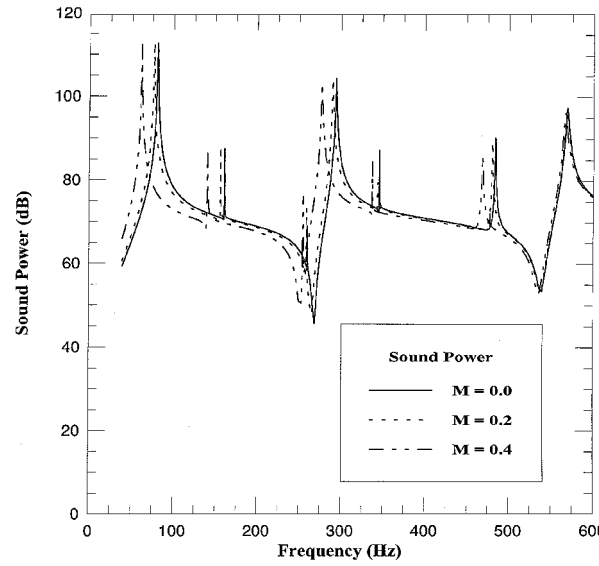

Fig. 5 Sound power of simply supported aluminum plate.

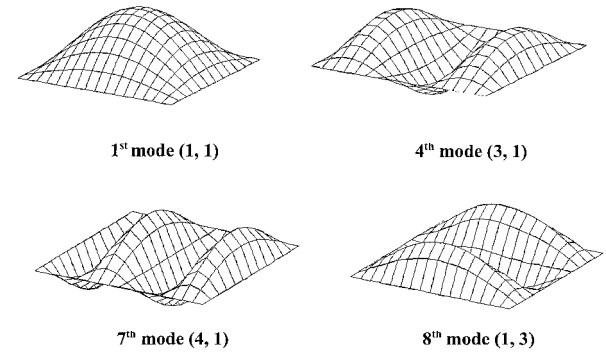

Fig. 6 Well-radiating mode shape of simply supported aluminum plate.

radiation efficiencies of each mode are calculated in Table 2. It is found that in the frequency range of 0–600 Hz the radiation efficiencies of the first, fourth, seventh, and eighth modes are much larger than those of the second, third, fifth, and sixth modes, which means that the first, fourth, seventh, and eighth modes (Fig. 6) radiate sound very well compared with the second, third, fifth, and sixth modes (Fig. 7). We also can observe this from Fig. 5, where the sound power in the frequency range of 0–600 Hz is dominated by the first, fourth, seventh, and eighth modes. This phenomenon can be explained by the first (1, 1), fourth (3, 1), and eighth (1, 3) modes being the odd–odd modes, which are the well-radiating modes, and the fifth mode (2, 2) being an even–even mode. The others are the odd–even and even–odd modes: the second (2, 1), third (1, 2), sixth (3, 2), and seventh (4, 1) modes. Unlike the second, third, and sixth modes, the seventh mode is an efficient radiator due to its high natural frequency. Therefore, if we design the sensors and actuators to minimize the response of well-radiating modes (first, fourth, seventh, and eighth modes), considering the effect of spillover on residual modes (second, third, fifth, and sixth modes),

Table 3 Modal force per unit voltage of optimized sensor for simply supported aluminum plate[a]

Mode	Modal force, N/V	Mode	Modal force, N/V
1 (1, 1)	$\mathbf{1.076 \times 10^{-3}}$	5, (2, 2)	7.927×10^{-13}
2 (2, 1)	1.565×10^{-5}	6 (3, 2)	4.674×10^{-12}
3 (1, 2)	-2.963×10^{-13}	**7 (4, 1)**	$\mathbf{-9.365 \times 10^{-4}}$
4 (3, 1)	$\mathbf{-1.427 \times 10^{-3}}$	**8 (1, 3)**	$\mathbf{1.829 \times 10^{-3}}$

[a]Boldfaced values are well-radiating modes.

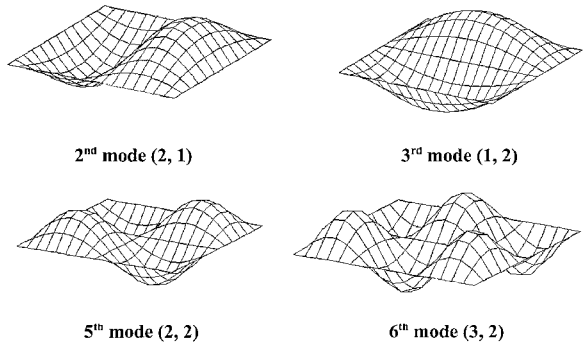

Fig. 7 Residual mode shape of simply supported aluminum plate.

Fig. 8 Optimal electrode shape of PVDF sensor on aluminum plate: controlled modes, first, fourth, seventh, and eighth; and uncontrolled modes, second, third, fifth, and sixth.

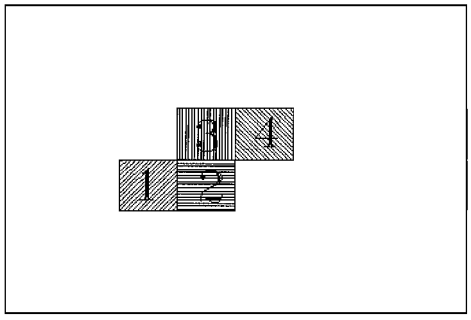

Fig. 9 Optimal placement of PZT actuators on aluminum plate: controlled modes, first, fourth, seventh, and eighth; and uncontrolled modes, second, third, fifth, and sixth.

we can achieve global noise reduction. The optimal electrode shape of the PVDF sensor and the optimal placement of PZT actuators are given in Figs. 8 and 9, respectively. During the design of the actuators, it is assumed that the size and the number of PZT actuators are constant, and in Fig. 9 the number of actuators is four. The genetic algorithm is used as an optimization method. Population in a generation is set to 1000. Probabilities of crossover and mutation are 0.9 and 0.01, respectively. Figure 10 shows the progress of the best fitness and the average fitness with generation. Improvement of the performance is obtained at the early stage. Modal forces of the optimized PVDF sensor are listed in Table 3. The difference in the modal force is observed between the controlled modes and the residual modes. The uncontrolled and controlled responses of sound power at $M = 0.0$ and 0.4 are shown in Figs. 11 and 12, respectively. It is clear that global noise reduction is realized using the described method.

Table 4 Material properties of carbon/epoxy

Property	Carbon/epoxy (HFG HT145/RS1222)
E_1, GPa	122.5
E_2, GPa	7.929
ν_{12}	0.329
G_{12}, GPa	3.585
Density, kg/m^3	1600
Thickness, mm	0.125

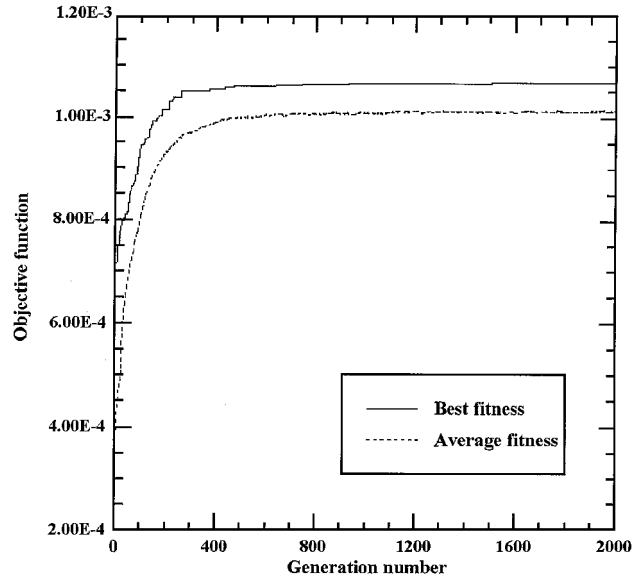

Fig. 10 Best and average fitness curve for sensor design.

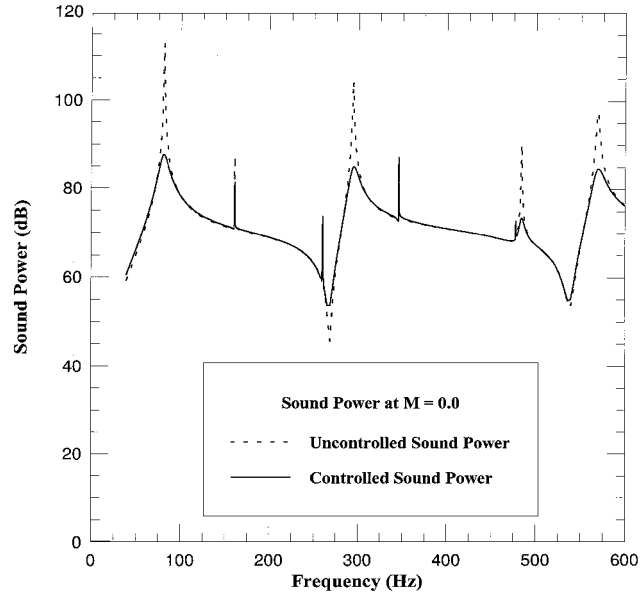

Fig. 11 Uncontrolled and controlled sound power ($M = 0.0$) for aluminum plate.

Control of Sound Fields from a Simply Supported Carbon/Epoxy Composite Plate in Flow

In this section, acoustic radiation from a simply supported composite plate on an infinite baffle is considered (Fig. 13). The excitation by disturbances is applied as in the aluminum case in the preceding section. It is also estimated that the mean flow speed is less than the flutter speed. The acoustic medium is air, whose density is 1.21 kg/m^3 and wave velocity is 343 m/s. The composite plate is made of carbon/epoxy composite, whose lamination sequence is $[0_3/45_3/-45_3/90_3]_s$. The material properties of the carbon/epoxy composite are summarized in Table 4. The dimensions of the composite plate are $0.6 \times 0.4 \times 0.003$ m. The material properties of PZT

Table 5 Natural frequency and radiation efficiency of simply supported composite plate with piezoelectric material, $M = 0.0$[a]

Mode	Frequency, Hz	Radiation efficiency
1 (1, 1)	55	$\mathbf{2.532 \times 10^{-2}}$
2 (2, 1)	134	6.491×10^{-3}
3 (1, 2)	150	4.531×10^{-3}
4 (2, 2)	227	1.707×10^{-3}
5 (3, 1)	271	$\mathbf{3.454 \times 10^{-2}}$
6 (1, 3)	312	$\mathbf{5.060 \times 10^{-2}}$
7 (3, 2)	353	8.270×10^{-3}
8 (2, 3)	394	2.671×10^{-2}
9 (4, 1)	462	$\mathbf{6.540 \times 10^{-2}}$

[a]Boldfaced values are well-radiating modes.

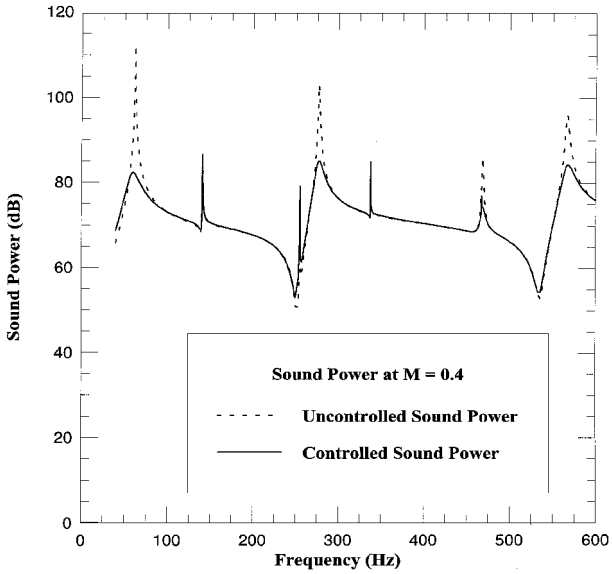

Fig. 12 Uncontrolled and controlled sound power ($M = 0.4$) for aluminum plate.

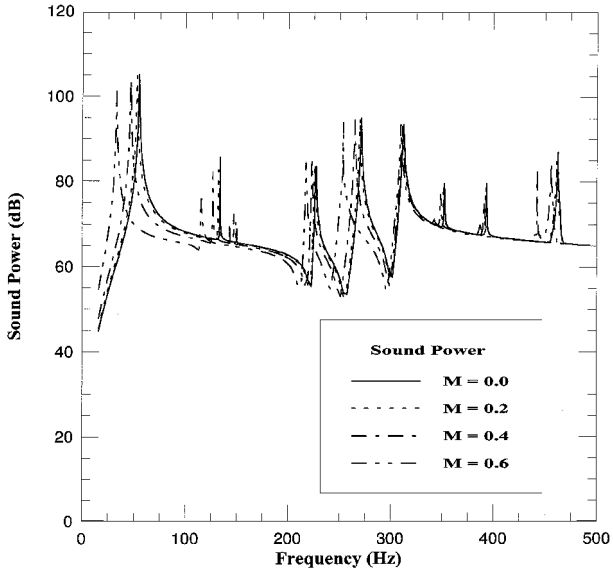

Fig. 13 Sound power of simply supported composite plate.

and PVDF are given in Table 1 (Refs. 16 and 17). From Fig. 13, reduction of the natural frequencies can be observed as the mean flow speed increases.

To select the controlled modes, the radiation efficiencies of each mode are calculated in Table 5. It is found that the radiation efficiencies of the first, fifth, sixth, and ninth modes are much higher than those of the second, third, fourth, seventh, and eighth modes.

This means that the first, fifth, sixth, and ninth modes (Fig. 14) radiate sound very well compared with the second, third, fourth,

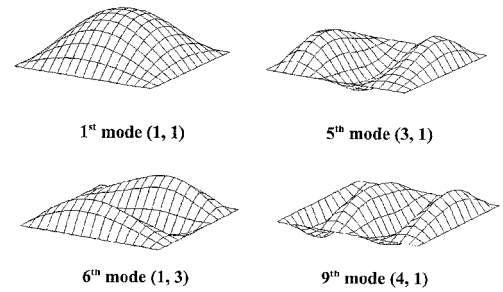

Fig. 14 Well-radiating mode shape of simply supported composite plate.

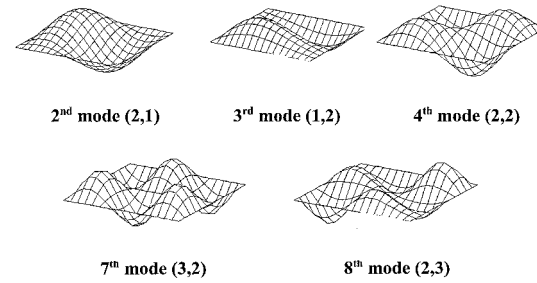

Fig. 15 Residual mode shape of simply supported composite plate.

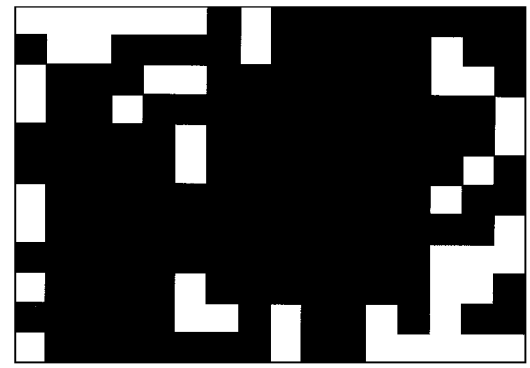

Fig. 16 Optimal electrode shape of PVDF sensor on composite plate: controlled modes, first, fifth, sixth, and ninth; and uncontrolled modes, second, third, fourth, seventh, and eighth.

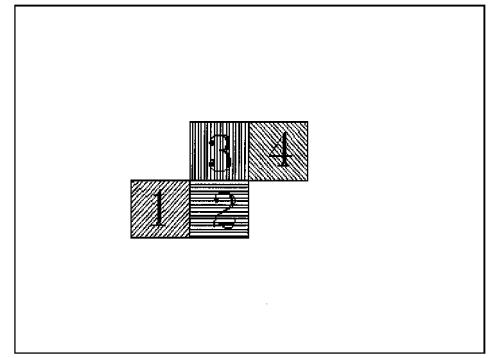

Fig. 17 Optimal placement of PZT actuators on composite plate: controlled modes, first, fifth, sixth, and ninth; and uncontrolled modes, second, third, fourth, seventh, and eighth.

seventh, and eighth modes (Fig. 15). This is different from the preceding case of an isotropic aluminum plate. We can observe that the first (1, 1), fifth (3, 1), and sixth (1, 3) modes are odd–odd modes, which are the well-radiating modes, and the fourth mode (2, 2) is an even–even mode. The second (2, 1), third (1, 2), seventh (3, 2), eighth (2, 3), and ninth (4, 1) modes are odd–even and even–odd modes. Unlike the second, third, seventh, and eighth modes, the ninth mode is selected as a controlled mode because it is an efficient radiator due to its high natural frequency. To suppress the sound fields, sensors and actuators should be designed to control the well-radiating

Table 6 Modal force per unit voltage of optimized sensor for simply supported carbon/epoxy composite plate[a]

Mode	Modal force, N/V	Mode	Modal force, N/V
1 (1, 1)	$\mathbf{1.083 \times 10^{-3}}$	**5 (3, 1)**	$\mathbf{-1.273 \times 10^{-3}}$
2 (2, 1)	3.817×10^{-7}	**6 (1, 3)**	$\mathbf{-1.382 \times 10^{-3}}$
3 (1, 2)	1.321×10^{-6}	7 (3, 2)	-9.533×10^{-7}
4 (2, 2)	-1.071×10^{-7}	8 (2, 3)	8.323×10^{-7}
		9 (4, 1)	$\mathbf{-1.129 \times 10^{-3}}$

[a]Boldfaced values are well-radiating modes.

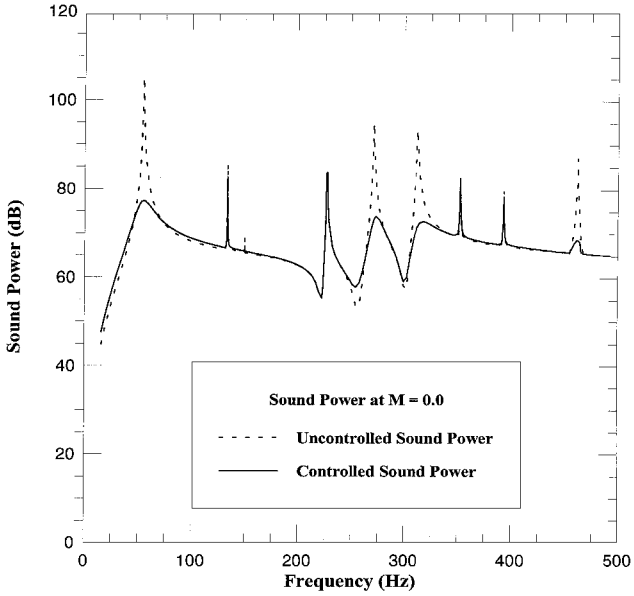

Fig. 18 Uncontrolled and controlled sound power ($M = 0.0$) for composite plate.

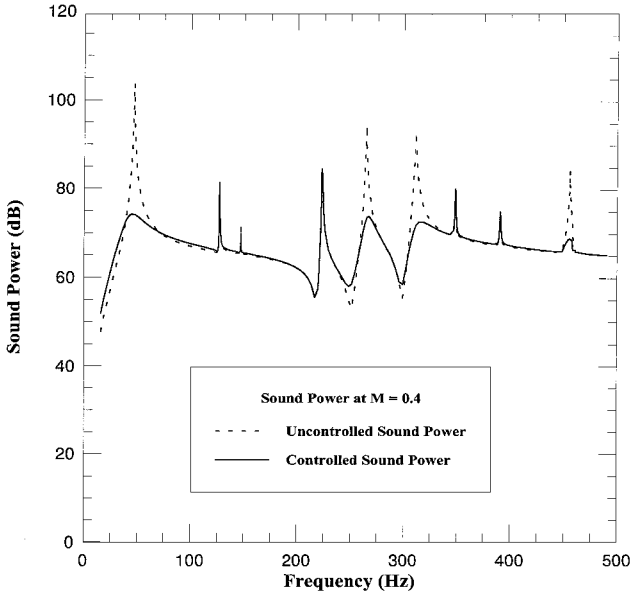

Fig. 19 Uncontrolled and controlled sound power ($M = 0.4$) for composite plate.

modes (first, fifth, sixth, and ninth modes), considering the effect of spillover on residual modes (second, third, fourth, seventh, and eighth modes). The optimal electrode shape of the PVDF sensor and the optimal placement of PZT actuators are given in Figs. 16 and 17, respectively. In the design of actuators, it is assumed that the size and number of PZT actuators are constant, and in Fig. 17, the number of actuators is four. The genetic algorithm is used as an optimization method. Modal forces of the optimized PVDF sensor are listed in Table 6. The difference in the modal force is observed between the controlled modes and the residual modes. The uncontrolled and controlled responses of sound power at $M = 0.0$ and 0.4 are shown in Figs. 18 and 19, respectively.

V. Conclusions

A numerical investigation of the control of the acoustic field from a plate in flow excited by disturbance is reported, considering the presence of piezoelectric sensor/actuators. When thin structures, such as plates or shells, are vibrating in flow, the natural frequencies are reduced compared with the case without flow. Also, it is found that some specific modes become very efficient radiators compared with other modes. Therefore, a specific control strategy is required for suppression of the global radiation field. The selection of controlled modes is a prerequisite because the number of modes that can be controlled simultaneously is limited. For structural acoustic control, the well-radiating modes should be the controlled modes. Radiation efficiency is used as a reference to select the controlled modes. Piezoelectric material is preferred to microphones as a sensor in this case because microphones are difficult to use in the radiation far field. The optimal electrode pattern of PVDF sensor and the optimal placement of PZT actuators are calculated by the genetic algorithm to minimize the well-radiating modes and to avoid the observation and control spillover. It is expected that global noise reduction can be realized by using the method and that this method can be extended to control the cabin noise of high-speed aircraft.

References

[1]Fuller, C. R., "Active Control of Sound Transmission/Radiation from Elastic Plates by Vibration Inputs: I. Analysis," *Journal of Sound and Vibration*, Vol. 136, No. 1, 1990, pp. 1–15.

[2]Atalla, N., and Nicolas, J., "A Formulation for Mean Flow Effects on Sound Radiation from Rectangular Baffled Plates with Arbitrary Boundary Conditions," *Symposium on Flow-Induced Vibration and Noise*, Vol. 3, NCA-Vol. 13, American Society of Mechanical Engineers, New York, 1992, pp. 69–84.

[3]Fahy, F., *Sound and Structural Vibration: Radiation, Transmission and Response*, Academic, New York, 1985, pp. 53–142.

[4]Lee, C. K., "Piezoelectric Laminates: Theory for Distributed Sensors and Actuators," *Intelligent Structural Systems*, edited by H. S. Tzou and G. L. Anderson, Kluwer Academic, Norwell, MA, 1992, pp. 75–167.

[5]Wu, S. F., and Maestrello, L., "Responses of Finite Baffled Plate to Turbulent Flow Excitations," *AIAA Journal*, Vol. 33, No. 1, 1995, pp. 13–19.

[6]Hall, W. S., *The Boundary Element Method*, Kluwer Academic, Boston, MA, 1993, pp. 166–175.

[7]Kim, S. J., and Yoon, K. W., "Active Control of Sound Fields from a Composite Plate Using the Anisotropy and Shape of Distributed PVDF Actuators," *Journal of Sound and Vibration*, Vol. 202, No. 4, 1997, pp. 461–476.

[8]Clark, R. L., and Fuller, C. R., "Optimal Placement of Piezoelectric Actuators and Polyvinylidene Fluoride Error Sensors in Active Structural Acoustic Control Approaches," *Journal of the Acoustical Society of America*, Vol. 92, No. 3, 1992, pp. 1521–1533.

[9]Johnson, M. E., and Elliott, S. J., "Active Control of Sound Radiation Using Volume Velocity Cancellation," *Journal of the Acoustical Society of America*, Vol. 98, No. 4, 1995, pp. 2174–2186.

[10]Lee, H. K., and Park, Y. S., "A Near-Field Approach to Active Control of Sound Radiation from a Fluid-Loaded Rectangular Plate," *Journal of Sound and Vibration*, Vol. 196, No. 5, 1996, pp. 579–593.

[11]Song, L., Koopmann, G. H., and Fahnline, J. B., "Active Control of the Acoustic Radiation of a Vibrating Structure Using a Superposition Formulation," *Journal of the Acoustical Society of America*, Vol. 89, No. 6, 1991, pp. 2786–2792.

[12]Ryou, J. K., Park, K. Y., Kim, Y. H., and Kim, S. J., "Electrode Pattern Design of Piezoelectric Sensors and Actuators by Genetic Algorithm," *Proceedings of the AIAA/ASME/ASCE/AHS/ASC 38th Structures, Structural Dynamics, and Materials Conference*, AIAA, Reston, VA, 1997, pp. 1747–1754.

[13]Goldberg, D. E., *Genetic Algorithms in Search, Optimization & Machine Learning*, Addison–Wesley, Reading, MA, 1989, pp. 1–10.

[14]Lewis, F. L., *Applied Optimal Control and Estimation*, Prentice–Hall International, Upper Saddle River, NJ, 1992, pp. 526–547.

[15]Chang, Y. M., and Leehey, P., "Acoustic Impedance of Rectangular Panels," *Journal of Sound and Vibration*, Vol. 64, No. 2, 1979, pp. 243–256.

[16]*Product Catalog*, Piezo Systems, Inc., Cambridge, MA, 1993.

[17]*Kynar Piezo Film Technical Manual*, Pennwalt Corp., Valley Forge, PA, 1987.

G. M. Faeth
Editor-in-Chief